

INTERNATIONAL SOCIETY FOR SOIL MECHANICS AND GEOTECHNICAL ENGINEERING



This paper was downloaded from the Online Library of the International Society for Soil Mechanics and Geotechnical Engineering (ISSMGE). The library is available here:

<https://www.issmge.org/publications/online-library>

This is an open-access database that archives thousands of papers published under the Auspices of the ISSMGE and maintained by the Innovation and Development Committee of ISSMGE.

Three dimensional probabilistic slope stability analysis by RFEM

Trois dimensions probabiliste stabilité des talus par analyse RFEM

D.V. Griffiths & J. Huang
Colorado School of Mines, USA

G. A. Fenton
Dalhousie University, Canada

ABSTRACT

The paper investigates the probability of failure of 2-d and 3-d slopes using the Random Finite Element Method (RFEM). RFEM combines elastoplasticity with random field theory in a Monte-Carlo framework. It is found that 2-d probabilistic analysis, by implicitly assuming perfect spatial correlation in the third direction, may underestimate the probability of failure of slopes.

RÉSUMÉ

Le document examine la probabilité de défaillance de 2-d et 3-d en utilisant les pistes Random méthode des éléments finis (RFEM). RFEM combine l'élastoplasticité avec la théorie des champs aléatoires dans un Monte-Carlo cadre. Il se trouve que le 2-d probabilistic analysis, par parfaite supposer implicitement la corrélation spatiale dans la troisième direction, mai sous-estimer la probabilité de défaillance des pistes

Keywords : two dimensional, three dimensional, slope stability, finite element method, probability of failure, spatial correlation.

1 INTRODUCTION

A considerable number of studies (e.g. Duncan 1996) have compared the factor of safety from a full 3-d slope analysis (FS_3) with that obtained from a traditional 2-d analysis (FS_2) and concluded that in the majority of cases for rather uniform slopes $FS_3 / FS_2 \geq 1$. The assumption that 2-d analysis leads to conservative factors of safety needs some qualification however. Firstly, a conservative result may only be obtained if a "pessimistic" section in the 3-d problem is selected for 2-d analysis as shown by Griffiths and Huang (2008). In a slope that contains layering and strength variability in the third dimension, the choice of a 2-d "pessimistic" section may not be intuitively obvious.

In this paper we compare the probability of failure of 3-d and 2-d slopes involving highly variable soils using RFEM. At the time of writing, relatively few investigators have worked on 3-d slope reliability analysis. Important early work was reported by Vanmarcke (1977) which led other investigators to follow a similar framework. For example, Yücemem and Al-Homoud (1990) considered 3-d slope reliability incorporating a 1-d random field and some quite restrictive assumptions about the kinematics of the 3-d failure mechanism.

In this study, the Random Finite Element Method (RFEM) (Fenton and Griffiths 2008) combines 3-d elastoplastic finite elements and 3-d random field theory in a Monte-Carlo framework to directly assess the reliability of 3-d slopes. The influence of the out-of-plane dimension is assessed for different combinations of the coefficient of variation of strength and spatial correlation length. The 3-d results are compared with an equivalent 2-d probabilistic analysis by RFEM which assumes plane strain conditions and perfect correlation in the out-of-plane direction. It will be shown that under some conditions, 3-d analysis leads to higher probabilities of failure than 2d.

2 DETERMINISTIC ANALYSES

The method and programs of Griffiths and Lane (1999) and Griffiths and Marquez (2007) were used to analyse the stability of the 2-d and 3-d slopes presented in this paper.

The 2-d slope profile shown in Figure 1 uses 8-node plane strain finite elements to model a 2:1 undrained clay slope with strength parameters $\phi_u = 0$ and $C_u = c_u / (\gamma_{sat} H) = 0.167$. Using any standard slope stability analysis method it can be shown that $FS = 1.39$ (see e.g. Griffiths and Lane 1999).

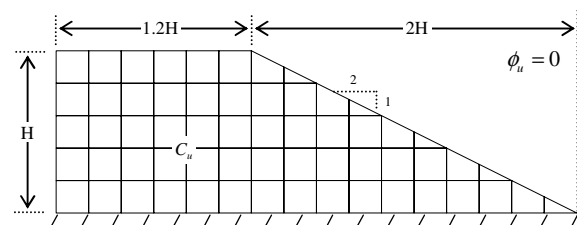


Figure 1. 2-d Finite element mesh

The 3-d slope profile, modeled using 20-node hexahedral elements shown in Figure 2, is of a uniform slope in which the cross-section of the slope shown in Figure 1 is extended by a distance L in the z direction. The bottom of the mesh ($y = -H$) and the sides ($z = 0$ and L) are fixed while the back ($x = 0$) is allowed to move only in the vertical plane. The depth L of the slope was varied in the range $0.8 < L/H < 12$ (because of symmetry the actual mesh depth was only half this amount), enabling an investigation to be made of the influence of three-dimensionality. A comparison of the factor of safety obtained in the 3-d and 2-d analyses is given in Figure 3. The factor of safety in 3-d was always higher than in 2-d but tended to the plane strain solution for depth ratios of the order of $L/H = 10$.

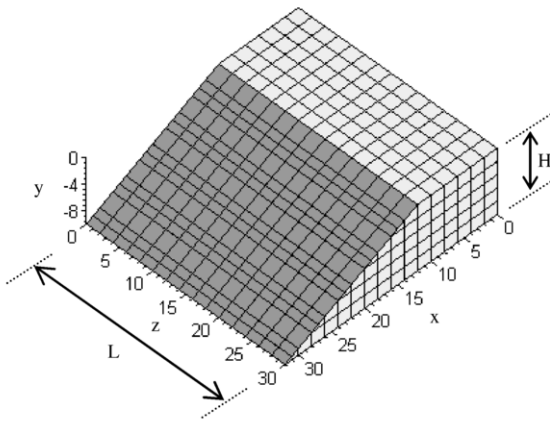


Figure 2. 3-d Finite element mesh

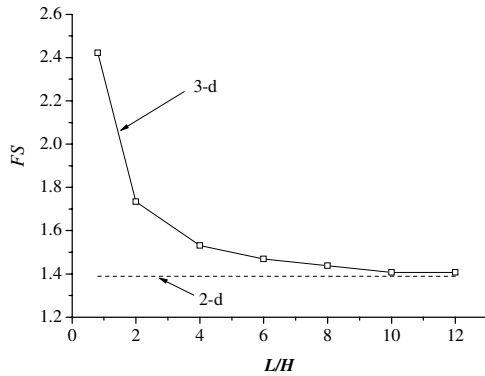


Figure 3. Comparison of 3-d and 2-d deterministic analyses

3 PROBABILISTIC DESCRIPTIONS OF STRENGTH PARAMETERS

In this study, the dimensionless shear strength parameter C_u is assumed to be a random variable characterized statistically by a lognormal distribution (i.e. the logarithm of the property is normally distributed). The lognormally distributed shear strength C_u has three parameters; the mean, μ_{C_u} , the standard deviation σ_{C_u} , and the spatial correlation length $\theta_{\ln C_u}$. The variability of C_u can conveniently be expressed by the dimensionless coefficient of variation defined as

$$v_{C_u} = \frac{\sigma_{C_u}}{\mu_{C_u}} \quad (1)$$

The parameters of the normal distribution (of the logarithm of C_u) can be obtained from the standard deviation and mean of C_u as follows:

$$\sigma_{\ln C_u} = \sqrt{\ln\{1+v_{C_u}^2\}} \quad (2)$$

$$\mu_{\ln C_u} = \ln \mu_{C_u} - \frac{1}{2} \sigma_{\ln C_u}^2 \quad (3)$$

A third parameter, the spatial correlation length $\theta_{\ln C_u}$, will also be considered in this study. Since the actual undrained shear strength field is assumed to be lognormally distributed, its logarithm yields an “underlying” normal distribution (or Gaussian) field. The spatial correlation length is measured with respect to $\ln C_u$. In particular, the spatial correlation length ($\theta_{\ln C_u}$) describes the distance over which the spatially random values will tend to be significantly correlated in the underlying Gaussian field. Thus, a large value of $\theta_{\ln C_u}$ will imply a smoothly varying field, while a small value will imply a ragged field. The random field is generated using local average subdivision method (see e.g. Fenton and Griffiths 2008).

In the current study, the spatial correlation length has been non-dimensionalized by dividing it by the height of the embankment H and will be expressed in the form,

$$\Theta_{C_u} = \theta_{\ln C_u} / H \quad (4)$$

4 SINGLE RANDOM VARIABLE APPROACH

Single random variable (SRV) probabilistic methods do not explicitly take account of the spatial variation, hence slopes are assumed to be uniform (spatially constant properties) with C_u selected randomly from a lognormal distribution. SRV probabilistic methods imply a spatial correlation length $\Theta_{C_u} = \infty$.

Since there is only one random variable in an undrained analysis and $FS \propto C_u$, $v_{FS} = v_{C_u}$ and the probability of failure (p_f) is simply equal to the probability that FS will be less than unity. Quantitatively, this equals the area beneath the probability density function of FS corresponding to $FS < 1$. For the slope shown in Figure 1 which has $\mu_{FS} = 1.39$ if we let $v_{C_u} = v_{FS} = 0.5$, Eqs. (2) and (3) give that the mean and standard deviation of the underlying normal distribution of $\ln FS$ as $\mu_{FS} = 0.218$ and $\sigma_{FS} = 0.472$ respectively. The probability of failure is therefore given by:

$$p_f = p[FS < 1] = \Phi\left(\frac{-\mu_{FS}}{\sigma_{FS}}\right) = 0.32 \quad (5)$$

where $\Phi(\cdot)$ is the cumulative standard normal distribution function.

5 RANDOM FINITE ELEMENT METHOD

The RFEM involves the generation and mapping of a random field of properties onto a finite element mesh. Full account is taken of local averaging and variance reduction over each element, and an exponentially decaying (Markov) spatial correlation function is incorporated. After application of gravity loads, if the algorithm is unable to converge within a user-defined iteration ceiling (see e.g. Griffiths and Lane 1999), the implication is that no stress distribution can be found that is simultaneously able to satisfy both the Mohr-Coulomb failure criterion and global equilibrium. If the algorithm is unable to satisfy these criteria, typically accompanied by a sudden increase in nodal displacements, failure is said to have occurred. The analysis is repeated numerous times using Monte-Carlo simulations. Each realization of the Monte-Carlo process involves the same underlying mean, standard deviation and spatial correlation length of soil properties, however the properties vary spatially from one realization to the next. Following a suite of Monte-carlo simulations, p_f can be easily estimated by dividing the number of simulations that failed by the total number of simulations. Although not implemented in the current paper, the analysis has the option of including cross correlation between properties and anisotropic spatial correlation lengths (e.g. the spatial correlation length in a naturally occurring stratum of soil is often higher in the horizontal direction).

6 PROBABILISTIC ANALYSES

The methodology described by Griffiths and Fenton (2004) for 2-d slope reliability has been extended to 3-d slopes in the current work. The boundary conditions are the same as in the deterministic case, however in the probabilistic analyses we have included the option of smooth side boundaries which means the sides ($z=0$ and L) are allowed to move only in the vertical plane.

Figures 4 and 5 show typical failed slopes with (isotropic) $\Theta_{C_u} = 2.0$ and $\Theta_{C_u} = 0.25$. It can be seen that failure, when it

occurs, involves a greater volume of soil when the spatial correlation length is smaller.

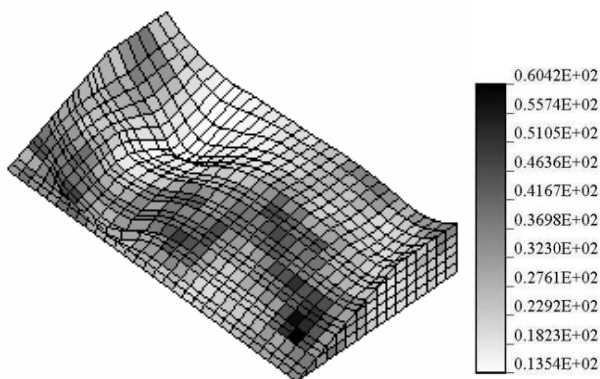


Figure 4. Slope failure with (isotropic) $\Theta_{c_s} = 2.0$ and rough boundary condition

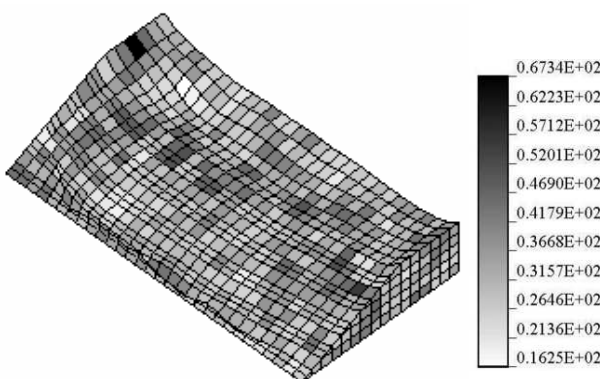


Figure 5. Slope failure with isotropic $\Theta_{c_s} = 0.25$ and rough boundary condition

Keeping $\Theta_{c_s} = 1.0$ and $v_{c_s} = 0.5$ fixed, the depth ratio was varied in the range $0.2 < L/H < 16$ to investigate the influence of three-dimensionality with results presented in Figure 6. In the case of smooth boundary conditions, the p_f of one slice ($L/H = 0.2$) in the 3-d analysis is equivalent to that given by a 2-d RFEM analysis with $p_f \approx 0.2$. It is also shown in the smooth case that as L/H is increased, p_f initially decreases to reach a minimum at about $L/H \approx 3$ before rising to eventually exceed the 2-d value at approximately $L/H > 10$.

In the rough case, p_f is close to zero for a narrow slice and increases continuously as L/H increases and exceeds the 2-d value by extrapolation at approximately $L/H > 18$. In both the rough and smooth cases it may be speculated that $p_f \rightarrow 1$ as $L/H \rightarrow \infty$. It is clear from Figure 6 that regardless of boundary conditions, the assumption of an infinite spatial correlation length in the third direction, implicit in any 2-d analysis, may underestimate p_f if the slope is long enough.

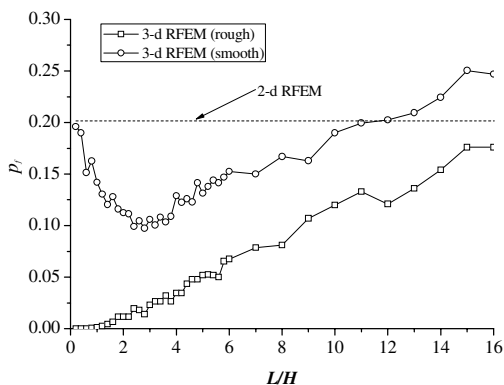


Figure 6. Probability of failure versus slope depths ($\Theta_{c_s} = 1.0, v_{c_s} = 0.5$)

Figure 7 presents further 3-d RFEM results showing the influence of spatial correlation length on p_f by varying Θ_{c_s} in the range $\Theta_{c_s} = \{0.125, 0.25, \dots, 2\}$. In this case the coefficient of variation of strength and the depth ratio have been fixed at $v_{c_s} = 0.5$ and $L/H = 6$ respectively. Also included in this figure is the result obtained by the SRV method and 2-d RFEM. It can be seen that compared to the 3-d analysis, the 2-d analysis underestimates the probability of failure when $\Theta_{c_s} > 1.5$ in the smooth case and $\Theta_{c_s} > 3.8$ in the rough case. As might be expected, both the 2-d and 3-d (smooth) RFEM analyses converge on the solution from the SRV method as Θ_{c_s} is increased.

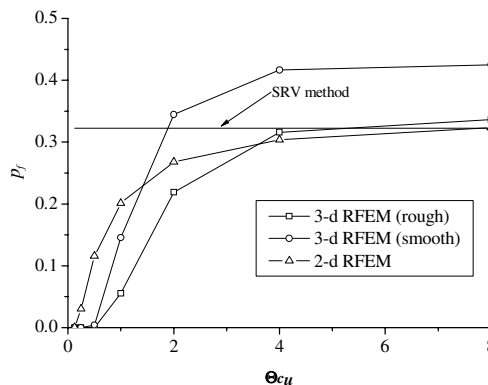


Figure 7. Probability of failure versus spatial correlation length ($L/H = 6, v_{c_s} = 0.5$)

The influence of increased strength variability was further investigated by setting $v_{c_s} = 1.0$ with results shown in Figures 8 and 9. Figure 8 shows a similar trend to that observed in Figure 6, however all the critical depth ratios are lower than those given when $v_{c_s} = 0.5$. For example 2-d ceases to be conservative when $L/H > 2.4$ in the smooth case and when $L/H > 4$ in the rough case (compared with $L/H > 10$ and $L/H > 18$ respectively when $v_{c_s} = 0.5$). Figure 8 also shows that the p_f with smooth boundary conditions reaches a minimum at $L/H = 1$ (compared with $L/H \approx 3$ when $v_{c_s} = 0.5$). The increased strength variability has resulted in the cross-over point (2-d RFEM analysis begins to give lower p_f than 3-d) occurring at lower depth ratios. It has also resulted in a faster convergence of the rough and smooth results with increased depth ratio. When $L/H > 15$, both rough and smooth cases gave essentially similar probabilities of failure with $p_f \rightarrow 1$.

Figure 9 shows that p_f from the 3-d RFEM analyses reaches a maximum at around $\Theta_{c_s} \approx 1.0$ for both rough and smooth boundary conditions. It can be anticipated that the p_f of 2-d and 3-d with smooth boundary condition will converge to the results obtained by the SRV when $\Theta_{c_s} \rightarrow \infty$. Similarly, as $\Theta_{c_s} \rightarrow \infty$, the 3-d p_f with rough boundary conditions will converge to the result obtained by the SRV method when $L/H > 10$ as predicted by the deterministic analyses.

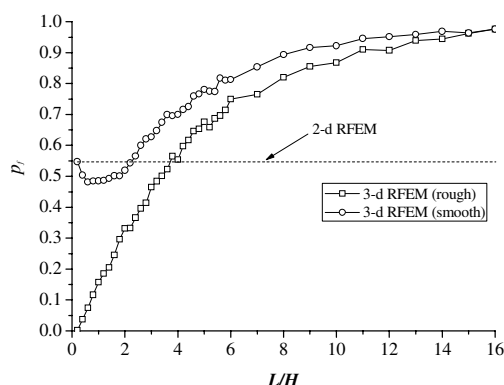


Figure 8. Probability of failure versus slope depths ($\Theta_{c_s} = 1.0, v_{c_s} = 1.0$)

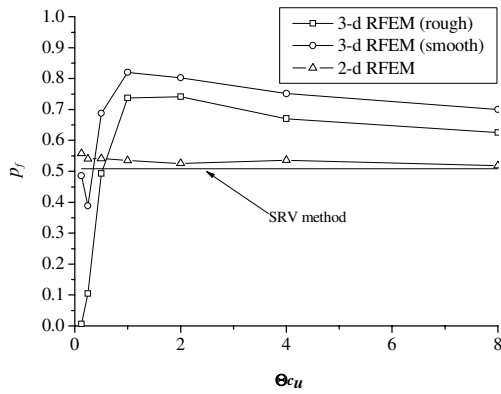


Figure 9. Probability of failure versus spatial correlation length ($L/H = 6, v_{c_s} = 1.0$)

The influence of spatial correlation length was further investigated by setting $\Theta_{c_s} = 2.0$. Figure 10 shows that 2-d ceases to be conservative when $L/H > 5$ for smooth boundary conditions (compared with $L/H = 10$ when $\Theta_{c_s} = 1.0$). The increased spatial correlation length has resulted in the cross-over point occurring at lower depth ratios.

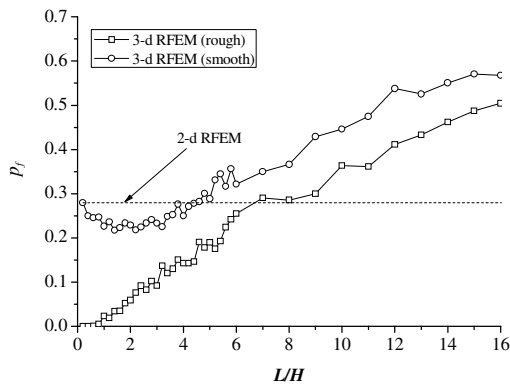


Figure 10. Probability of failure versus slope depths ($\Theta_{c_s} = 2.0, v_{c_s} = 0.5$)

Finally, Figures 11 and 12 show the influence of spatial correlation length on 2-d and 3-d RFEM probabilistic analysis of “short” ($L/H = 1$) and “long” ($L/H = 12$) slopes. For the case of $v_{c_s} = 0.5$, it can be seen that 2-d probabilistic analysis is always conservative for short slopes but may lead to unconservative probabilistic estimates for long slopes.

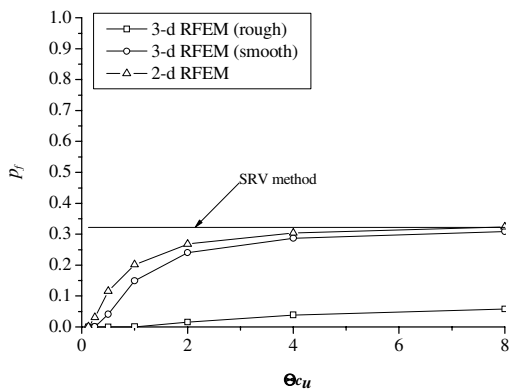


Figure 11. Probability of failure versus spatial correlation lengths ($L/H = 1, v_{c_s} = 0.5$)

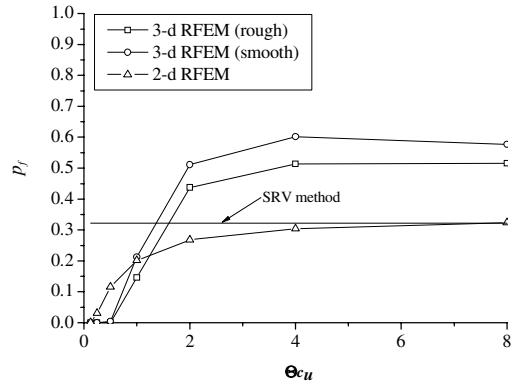


Figure 12. Probability of failure versus spatial correlation lengths ($L/H = 12, v_{c_s} = 0.5$)

7 CONCLUDING REMARKS

The paper has investigated the probability of slope failure using both 2-d and 3-d RFEM probabilistic analysis. The main conclusion is that by implicitly assuming an infinite spatial correlation in the third direction 2-d (plane strain) probability analysis may underestimate the probability of failure of slopes. This is counter to the usual assumption in regular slope stability analysis in which 2-d analysis is generally expected to give a conservative factor of safety. When performing probabilistic analysis of slopes, spatial variability in the out-of-plane direction must be properly considered to avoid unconservative designs for long slope.

ACKNOWLEDGEMENT

The authors wish to acknowledge the support of NSF grant CMS-0408150 on “Advanced probabilistic analysis of stability problems in geotechnical engineering”.

REFERENCES

Duncan, J. M. 1996. State of the art: Limit equilibrium and finite-element analysis of slopes. *ASCE Journal of Geotechnical Engineering*, Vol. 122, No. 7, pp.577-596.

Fenton, G. A., and Griffiths, D. V., 2008. Risk Assessment in Geotechnical Engineering. John Wiley & Sons, New York.

Griffiths, D. V., and Fenton, G. A. 2004. “Probabilistic slope stability analysis by finite elements.” *ASCE Journal of Geotechnical and Geoenvironmental Engineering*, Vol. 130, No. 5, pp.507-518.

Griffiths, D. V. and Lane, P. A. 1999. Slope stability analysis by finite elements. *Géotechnique* Vol. 49, No. 3, pp.387-403.

Griffiths D.V. and Huang, J. 2008. Reply to discussion by P.R. Vaughan on, “Three-dimensional slope stability analysis by elasto-plastic finite elements”, *Géotechnique* Vol. 58, No. 8, pp.683-685

Griffiths, D. V. and Marquez, R. M. 2007. Three-dimensional slope stability analysis by elasto-plastic finite elements. *Géotechnique* Vol. 57, No. 6, pp.537-546.

Vanmarcke, E. H. 1977. Reliability of earth slopes. *J Geotech Eng, ASCE*, Vol. 103, No. 11, pp.1247-1265.

Yucemen MS, Al-Homoud AS. 1990. Probabilistic three dimensional stability analysis of slopes, *Structural safety*, Vol. 12, No. 1, pp.1-20.